American Mineralogist, Volume 76, pages 1134–1140, 1991

Tetrahedrally coordinated Ti^{4+} in synthetic Ti-rich potassic richterite: Evidence from XRD, FTIR, and Raman studies

Giancarlo Della Ventura
Dipartimento Scienze della Terra, Sezione Mineralogico-Cristallografica, Università "La Sapienza," P. Aldo Moro 5, Rome I-00185, Italy

Jean-Louis Robert, Jean-Michel Bény
GS CNRS-BRGM, 1A rue de la Férollerie, F-45071 Orléans Cedex 2, France

Abstract

Samples have been prepared at 1 kbar P_{H_2O} for the join richterite–titanium richterite in the system K_2O-Na_2O-CaO-MgO-TiO_2-SiO_2-H_2O. Experimental results indicate that the Ti solubility strongly depends on temperature: it increases from 0.2 to about 0.8 atom per formula unit between 600 °C and 800 °C; no further increase is observed from 800 °C to 900 °C. Both FTIR and Raman spectroscopic data indicate that Ti^{4+} is entirely incorporated in tetrahedral sites. No significant change is observed in the OH-stretching region, indicating that Ti^{4+} is not bonded to OH groups. Only the Si-O stretching region is affected by Ti^{4+}, with band shifts closely corresponding to the calculated shift factor (0.92) for a $^{[4]}Si \rightarrow {}^{[4]}Ti$ substitution. The substitutional mechanism responsible for Ti incorporation is the direct isovalent substitution $Si^{4+} \rightarrow Ti^{4+}$. The progressive decrease in the tremolite-type band in the OH-stretching region with increasing Ti content confirms that the A-site cation splitting over A subsites is a function of the geometry of the A cavity, controlled by the major cationic substitutions. Powder XRD data for synthetic single-phase Ti-rich richterite reflect a regular increase in *a, b, c,* and β as a function of the Ti content, in response to the replacement of the small Si^{4+} ion (0.26 Å) by the larger Ti^{4+} ion (0.42 Å).

Introduction

X-ray single crystal studies of clinoamphibole crystal chemical relations that were carried out up to the middle of the 1970s resulted in assignment of all high-charge cations (charge $> 2^+$) present in the octahedral strip to the small OH-free M2 octahedron (see Hawthorne, 1981, for a compilation). These conclusions were based essentially on size considerations. During the last decade, more detailed analyses, performed primarily by means of infrared spectrometry, have demonstrated several exceptions to this relation (Semet, 1973; Robert, 1981).

Ti^{4+} represents a peculiar case. Ti-rich amphiboles belong to two different groups: the hornblende-type (kaersutite) and the richterite-type amphiboles. In potassium richterite, the Ti content may be up to 6–7 wt% TiO_2; that corresponds approximately to 0.7 Ti atom per formula unit (pfu) (Wagner and Velde, 1986).

Several substitutional mechanisms have been proposed to explain the presence of such high amounts of Ti in the amphibole structure. They may be summarized as follows:

1. $^{[6]}Al, {}^{[4]}Si \rightleftharpoons {}^{[6]}Ti, {}^{[4]}Al$, the Tschermak substitution (Helz, 1973). This mechanism is theoretically possible to some extent for hornblende. For example, in pargasite $NaCa_2(Mg_4Al)(Si_6Al_2)O_{22}(OH)_2$, the Ti end-member derived by the above exchange equation would lead to the end-member $NaCa_2(Mg_4Ti)(Si_5Al_3)O_{22}(OH)_2$, which is very similar to the formula of sadanagaite (Shimazaki et al., 1984).

2. $^{[6]}Al, OH^- \rightleftharpoons {}^{[6]}Ti, O^{2-}$, a mechanism involving deprotonation. Oxy-kaersutite is common in nature, and partial deprotonation related to Ti incorporation was suggested by Oba et al. (1982) for synthetic kaersutite. Structure refinements of natural oxy-kaersutite samples indicate the presence of substantial Ti in M1 (Kitamura et al., 1975). M1 is coordinated in part by OH in OH-bearing amphibole.

3. $2^{[6]}Mg \rightleftharpoons {}^{[6]}Ti, {}^{[6]}\square$. This reaction would generate an octahedral vacancy; it is well documented for structurally related Ti-rich phlogopite (Forbes and Flower, 1974). This mechanism seems theoretically possible in amphiboles but has never been documented, and there is no evidence for octahedral vacancies.

4. $^{[4]}Si \rightleftharpoons {}^{[4]}Ti$, which represents a direct isovalent substitution involving only tetrahedral sites. This mechanism was suggested for Ti-rich richterite found in lamproites (Wagner and Velde, 1986) on the basis of their calculated tetrahedral site deficiencies. Tetrahedrally coordinated Ti was inferred on the basis of single-crystal XRD data for natural Ti-rich richterite by Ungaretti (1980); it is known in other silicates, such as some natural garnets (Huggins et al., 1977). The existence of Ti^{4+} in fourfold coordination is still debated (Hartman, 1969; Waychunas, 1987).

0003–004X/91/0708–1134$02.00

In order to study the mechanism responsible for Ti^{4+} substitution in the richterite structure, a series of synthetic phases that have compositions along the join richterite–titanium richterite $[K(NaCa)Mg_5Si_8O_{22}(OH)_2]$-$[K(NaCa)Mg_5(Si_7Ti)O_{22}(OH)_2]$ has been investigated. This series was chosen because analytical data for naturally occurring Ti-rich potassium richterite indicate that the $^{[4]}Si \rightleftharpoons {}^{[4]}Ti$ substitution seems the most likely (Wagner and Velde, 1986). Starting compositions were separated by increments of 20 mol% along this join. Infrared and Raman spectroscopic techniques were then used in order to define Ti^{4+} sites and to characterize structural variations caused by the incorporation of Ti. Raman and IR spectroscopic methods are increasingly recognized as useful tools in deriving cation site occupancies for amphiboles, especially if high-charge cations are present (Semet, 1973; Raudsepp et al., 1987; Robert et al., 1989; Della Ventura and Robert, 1990).

Experimental methods

The starting materials used in the syntheses were silicate gels prepared according to the method of Hamilton and Henderson (1968). Ti was added to the gels as TiO_2 (anatase). The starting materials and distilled H_2O were inserted into noble metal capsules (Au for experiments at temperatures up to 800 °C and Pt above 800 °C) sealed by arc welding. A constant H_2O/gel ratio of 0.15 by weight was used for all experiments.

Experiments at 600 °C, 1 kbar and below were performed in Tuttle-type cold-seal externally heated pressure vessels, whereas experiments at 800 °C, 1 kbar were performed in Morey-type hot-seal externally heated vessels. Experiments at 900 °C, 1 kbar were performed in internally heated vessels, using Ar as a pressure medium. Estimated uncertainties for temperatures and pressures are ±5 °C and 50 bars, respectively. Standard experiment durations were 2 weeks at 600 °C, 5 d at 800 °C, and 3 d at 900 °C. Some long duration experiments (up to 6 weeks) were also performed at 600 °C, 1 kbar; they produced the same results as experiments performed at the same *PT* conditions for two weeks.

All products were studied by X-ray diffraction and optical techniques. Cell parameters were determined using data from X-ray powder patterns obtained with a Seifert Pad II automatic diffractometer, using ASTM Si as an internal standard. The powder patterns were fully indexed in space group $C2/m$ using the Appleman and Evans (1973) least-squares program. The final cell dimensions were refined using sets of 25–30 unambiguously indexed lines. Products were also examined by SEM, using a Cambridge Stereoscan 250 MK II electron microscope equipped with a Tracor, TN 2000 Si(Li) detector. High-resolution infrared spectra of the OH-stretching region (3750–3500 cm^{-1}) were recorded on a Perkin-Elmer 1760 FTIR spectrophotometer. Scanning conditions were 1-cm^{-1} nominal resolution, normal Beer-Norton apodization function, and scan speed of 0.2 cm^{-1}/s. Samples were prepared as KBr pellets, with a mineral to KBr ratio of 0.10 by weight. Details of IR sample preparation may be found in Robert et al. (1989). Raman spectra were recorded on a Jobin-Yvon U1000 spectrometer equipped with an Ar-ion laser, λ_0 = 488 nm; the uncertainty for peak positions is 1 cm^{-1}.

Table 1. Experimental conditions and products

Composition	Temperature (°C)	Pressure (bars)	Time (h)	Experimental product
0.0	600	1000	360	amph.
0.2	600	1000	360	amph. s.s.
0.4	600	1000	360	amph. s.s. + mica + ti.
0.6	600	1000	360	amph. s.s. + mica + ti.
0.8	600	1000	360	amph. s.s. + mica + ti.
1.0	600	1000	360	amph. s.s. + mica + ti.
0.0	800	1000	120	amph.
0.2	800	1000	120	amph. s.s.
0.4	800	1000	120	amph. s.s.
0.6	800	1000	120	amph. s.s.
0.8	800	1000	120	amph. s.s. + (pr.)
1.0	800	1000	120	amph. s.s. + (pr.)
0.2	900	1000	72	amph. s.s.
0.4	900	1000	72	amph. s.s.
0.6	900	1000	72	amph. s.s.
0.8	900	1000	72	amph. s.s. + (pr.)
1.0	900	1000	72	amph. s.s. + (pr.)

Note: Starting compositions are expressed in terms of Ti atoms per formula unit in the starting amphibole composition. Amph. s.s. = amphibole solid solution, ti. = titanite, pr. = priderite.

Experimental products and X-ray powder data

As the limits of Ti substitution in silicates increase with increasing temperature (see Robert, 1976, for phlogopite; Monier and Robert, 1986, for muscovite; Wagner and Velde, 1986, for potassium richterite), this first set of experiments was carried out with constant water pressure of 1 kbar and temperatures equal to 600 °C, 800 °C, and 900 °C.

Table 1 lists synthesis products. At 600 °C, 1 kbar, only compositions with Ti < 0.4 atom pfu gave a single amphibole. For Ti ≥ 0.4 atom pfu, assemblages consisting of amphibole plus mica plus titanite ($CaTiSiO_5$) were observed. X-ray data for the mica and chemical considerations based on the bulk starting compositions suggest that this Al-free mica is close to $K(Mg_{2.5}\square_{0.5})Si_4O_{10}(OH)_2$ in composition (Seifert and Schreyer, 1971).

At 800 °C, 1 kbar, a single amphibole is obtained for Ti ≤ 0.6 atom pfu. For higher Ti contents, small amounts of an additional phase related to priderite ($K_2MgTi_7O_{16}$; Dubeau and Edgar, 1985) were found with amphibole. This phase was identified both by X-ray diffraction and by SEM; additionally, some grains of titanite were detected by SEM, but XRD data could not confirm this observation. It is worth noting that, in nature, priderite has often been reported to occur in association with potassium richterite, e.g., in highly potassic lavas (Prider, 1939; Jaques et al., 1984; Carmichael, 1967; Kuehner et al., 1981; Wagner and Velde, 1986). Experiments at 900 °C, 1 kbar gave essentially the same results for the extent of the solid solution.

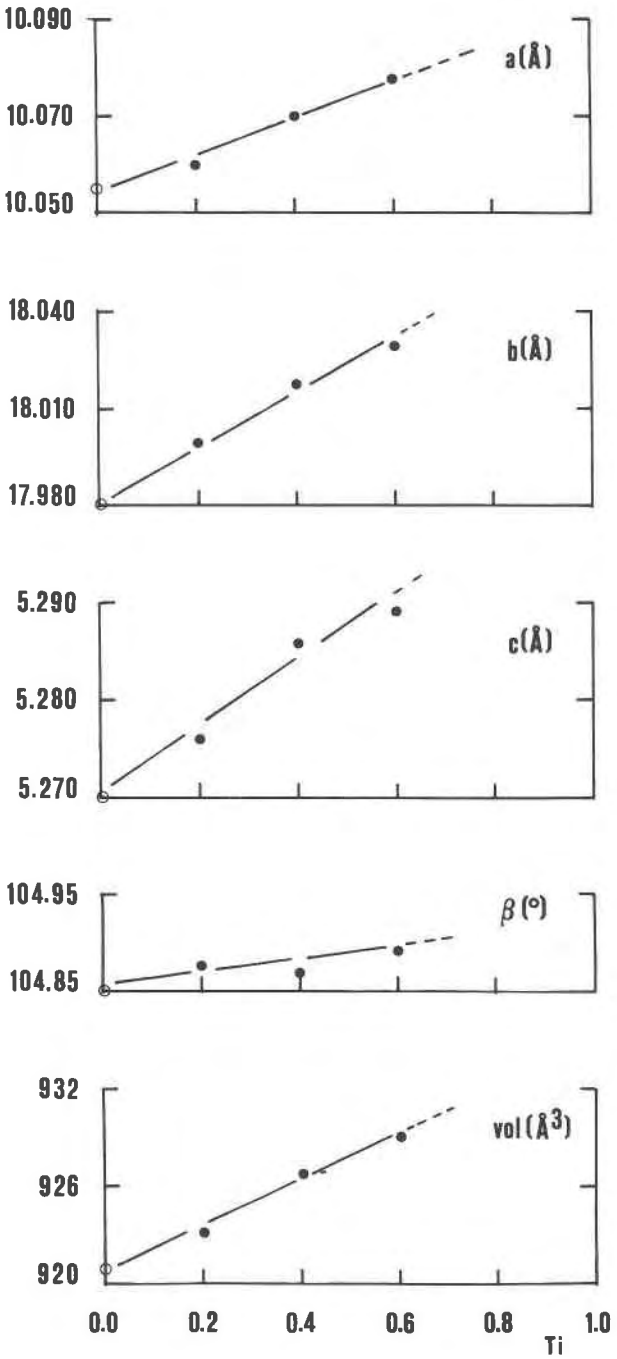

Fig. 1. Variation of cell parameters and cell volumes of synthetic potassium richterite samples prepared at 800 °C, 1 kbar in the single phase titanium richterite range, as a function of their Ti^{4+} content given in atoms per formula unit. Open circles: end-member potassium richterite, data from Robert et al. (1989). Full circles: this study.

Cell parameter variations for richterite as a function of experimentally controlled cation substitutions are available only for Na-K substitution in the A site (Huebner and Papike, 1970), OH-F substitution in the O3 site (Robert et al., 1989), and Mg-Fe substitution in the octahedral strip (Charles, 1975). Additional data on F end-members for both sodic and potassic richterite were given by Huebner and Papike (1970) and Cameron et al. (1983), whereas data related to Ca-Sr substitution in the M4 site for both sodic and potassic richterite were given by Della Ventura and Robert (1990).

Table 2. Cell dimensions and cell volumes of synthetic titanium richterite

Composition	a (Å)	b (Å)	c (Å)	β (°)	V (Å³)
0.0	10.055(1)	17.980(4)	5.270(1)	104.85(1)	921.0(2)
0.2	10.060(1)	18.000(2)	5.276(1)	104.88(1)	923.5(3)
0.4	10.070(1)	18.017(3)	5.286(1)	104.87(1)	927.0(3)
0.6	10.078(2)	18.030(3)	5.289(2)	104.89(2)	928.9(4)
0.8*	10.086(2)	18.042(4)	5.300(2)	104.89(2)	932.1(4)
1.0*	10.085(2)	18.029(5)	5.303(2)	104.94(2)	931.7(5)

Note: Cell parameters of Ti-rich potassic richterite samples synthesized at 800 °C, 1 kbar. Compositions are given in terms of Ti atom per formula unit in the amphibole. Numbers in parentheses are the estimated standard deviation to the last digit. Data for Ti-free richterite are from Robert et al. (1989).

* Two-phase assemblage, Ti-rich richterite and minor priderite.

The measured cell parameters of amphiboles synthesized at 800 °C, 1 kbar are listed in Table 2. Figure 1 shows cell parameter variations as a function of Ti content. Data points do not show significant deviation from a linear relationship for values from Ti = 0.0 to Ti = 0.6 atom pfu, supporting our inference that a continuous solid solution exists in this range. It should be noted that the cell parameters continue to increase for specimens with Ti = 0.6 to Ti = 0.8 atoms pfu in their bulk compositions, despite the presence of the accessory phase priderite observed for syntheses with Ti ≥ 0.8. We therefore conclude that the upper substitution limit of Ti^{4+} in our potassium richterite syntheses is very close to 0.8 apfu. As might be expected, the substitution of [4]Ti (ionic radius = 0.42 Å) for [4]Si (ionic radius = 0.26 Å) of (radii from Shannon, 1976), results in an overall expansion of the structure. All cell dimensions increase, including *c*, which is usually constant for all substitutions in Fe-free richterite samples and, in general, in Al-free amphiboles (Della Ventura and Robert, 1990).

FTIR spectroscopy measurements in the OH-stretching region

FTIR spectra of the OH-stretching region of Ti-bearing richterite samples are shown in Figure 2. The first spectrum, for Ti-free potassic richterite, was given by Robert et al. (1989). It shows a principal, high-wavenumber band at 3735 cm^{-1} and a minor tremolite-type band centered at 3670 cm^{-1}. The splitting of the first, high-intensity band into two components at 3735 and 3730 cm^{-1} has been discussed in Robert et al. (1989) and assigned to OH groups directed toward K ions almost equally disordered over the two A(*m*) and A(2/*m*) special positions. The tremolite-type band at 3670 cm^{-1} has been discussed both in terms of possible vacancies in A sites and of positional

disorder of alkali cations over A subsites (Robert et al., 1989; Della Ventura and Robert, 1990).

Spectra for samples with Ti = 0.2 to Ti = 0.6 atom per formula unit (that is, in the single phase range), show a progressive decrease in intensity of the 3735 cm^{-1} component assigned to a MgMgMg-OH → A(m) configuration relative to the 3730 cm^{-1} component assigned to the MgMgMg-OH → A(2/m) configuration (Robert et al., 1989). At the same time, the intensity of the 3670 cm^{-1} band progressively decreases, and there is increasing complexity of the main stretching band, with the appearence of at least two shoulders toward the low-wavenumber side, centered around 3728 cm^{-1} (observed for Ti = 0.4 apfu) and 3710 cm^{-1} (observed from Ti = 0.2 apfu).

These observations rule out the presence of Ti^{4+} in M1 or M3 octahedra bonded to an OH group, which would correspond to a total charge of +8, contributed by the three cations adjacent to the OH group. Few data are available for OH-stretching wavenumbers of hydroxyl groups bonded to three cations with a total change of +7 (Semet, 1973; Robert, 1981; Raudsepp et al., 1987). No data are available for the OH-stretching wavenumber of OH bonded to 2Mg + 1Ti in amphiboles. An example is known in the structurally related trioctahedral micas: in high-Ti phlogopite, the OH-stretching wavenumber (ν-OH) is close to 3640 cm^{-1}; in this phase, hydroxyl ions are bonded to 2Mg + 1Ti.

The decrease in intensity of the 3735 and 3730 cm^{-1} doublet to a point where it is not observable is consistent with a progressive migration of the K ion from the A(m) site to the central A(2/m) position as the Ti content increases.

Figure 1 illustrates the expansion in all lattice parameters with increasing Ti content. Following the model already proposed by Robert et al. (1989), we conclude that, owing to a larger A site, the splitting of the K ion site into two positions is not required. In other words, in the present case, the A-cation positional disorder may be interpreted as a function of the local polyhedral geometry in addition to factors proposed by previous authors (see Docka et al., 1987, for a compilation).

The progressive decrease in intensity of the 3670 cm^{-1} band suggests that even the overall occupancy of the A site is a consequence of the polyhedral geometry. Robert et al. (1989) have discussed the possibility that the tremolite-type band in synthetic and natural richterite samples must be assigned to an amphibole component with a vacant A site.

On the basis of careful experiments carried out to prevent any alkali leaching during syntheses, those authors concluded that, at least for the experimental conditions used (600 °C, 800 °C, 1 kbar), the presence of apparently vacant A sites in richterite could be explained by local geometrical constraints, especially the delocalization of the A cation over A(2/m) and A(m) subsites. The same argument has been proposed by Della Ventura and Robert (1990) for Sr-rich synthetic richterite. The present data provide us with additional arguments to support the previous conclusions: [4]Ti for [4]Si substitution causes expansion of the structure that allows the alkali cations to progressively fill the A(2/m) site.

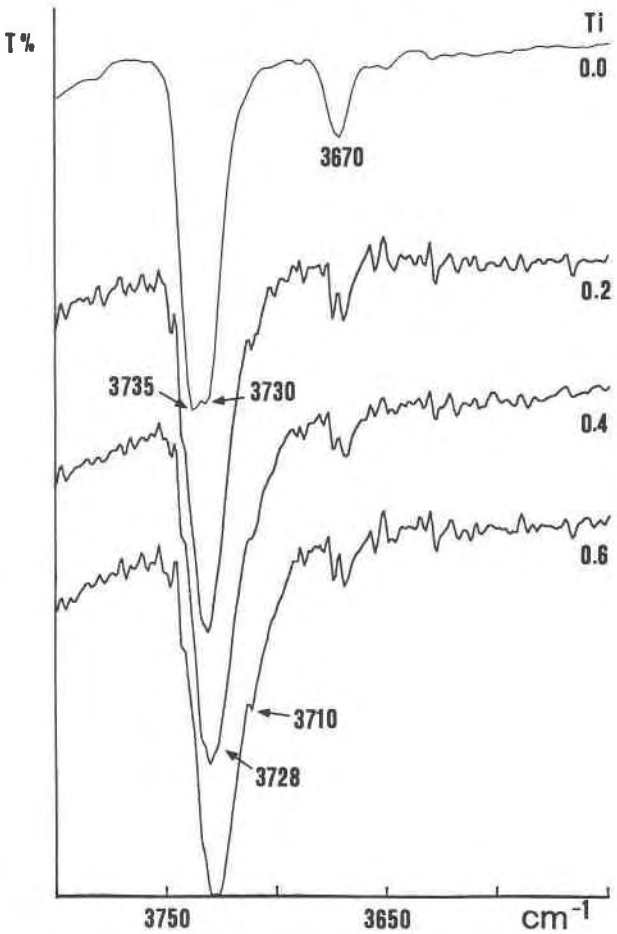

Fig. 2. Evolution of IR spectra of synthetic potassium richterite samples, with increasing Ti^{4+} content (in apfu) in the OH-stretching region.

The present state of the art does not permit unequivocal assignment of the new 3728 and 3710 cm^{-1} shoulders. Such minor wavenumber shifts cannot be assigned to any major change in the charge balance around the proton. Negative OH-stretching wavenumber shifts imply increased interaction between the OH proton and nearest neighbor O atoms (Della Ventura and Robert, 1990) and less repulsive interaction between the OH proton and K in the A(m) site (Robert et al., 1989). In the present case, the cause of these minor low-wavenumber shifts must be found in a second nearest-neighbor effect related to changes in the polyhedral geometry produced by substitution of Ti^{4+} for Si^{4+} and to the resulting increased regularity of the A site.

These infrared data also rule out the presence of Ti^{4+} in the OH-free octahedron M2 because such occupancy would imply an equivalent amount of tetrahedrally coordinated Mg^{2+} to maintain full occupancy of tetrahedra;

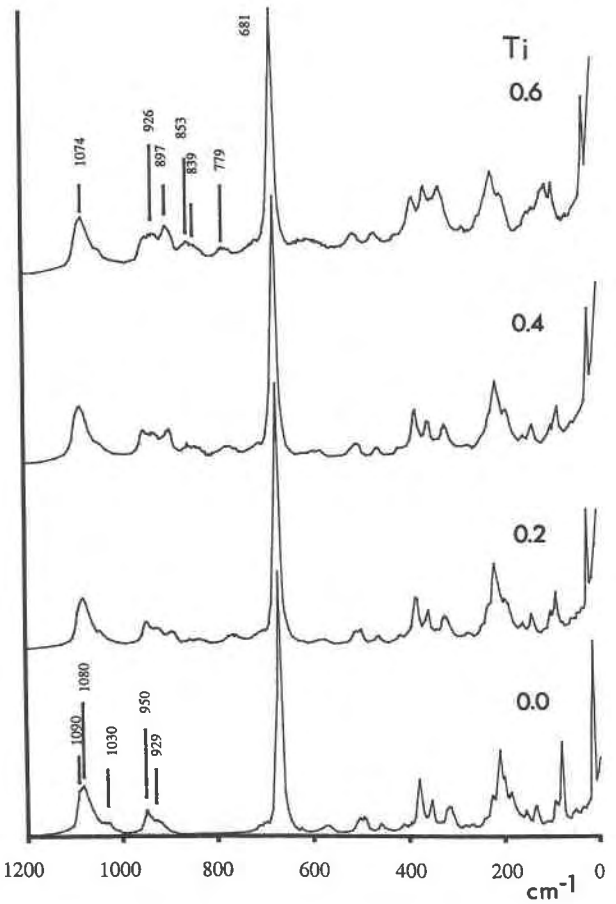

Fig. 3. Evolution of Raman spectra of synthetic potassium richterite, with increasing Ti^{4+} content (in apfu) in the range 1200–0 cm^{-1}.

the structural formula of the theoretically corresponding end-member would be $K(NaCa)(Mg_4Ti)(Si_7Mg)O_{22}(OH)_2$. An example of a tetrahedrally coordinated divalent cation in amphibole (Be^{2+}) is known only in joesmithite, $(Ca,Pb)Ca_2(M^{2+})_5(Si_6Be_2)O_{22}(OH)_2$ (Moore, 1969). However, other occurrences are provided by trioctahedral micas related to phlogopite (Seifert and Schreyer, 1971; Tateyama et al., 1976; Robert, 1981).

In trioctahedral micas containing a tetrahedrally coordinated divalent cation, a negative OH-stretching wavenumber shift (up to $\approx$35 cm^{-1}) is observed (Tateyama et al., 1976; Robert and Kodama, 1988) resulting from increasing interaction through H bonding between the OH proton and the underbonded O atoms of $(M^{2+}O_6)$ octahedra; furthermore, a significant broadening of the corresponding OH-stretching band is observed (Robert, 1981). The similarities between local environments of the OH dipole in clinoamphiboles and trioctahedral micas lead us to expect a similar behavior in tetrahedrally coordinated Mg in Ti-rich richterite; however, that is not observed. We therefore conclude that Ti^{4+} is entirely incorporated in the fourfold coordinated sites.

Raman scattering data

In the OH-stretching region, Raman scattering gives the same results as FTIR spectra; because this is common in amphiboles, these results are not given.

The evolution of the Raman spectrum in the wavenumber range 1200–0 cm^{-1} as a function of Ti content is represented in Figure 3. No data are available concerning the interpretation of Raman spectra of clinoamphiboles with filled A sites. In a recent paper, Gillet et al. (1989) discussed the Raman spectrum of glaucophane $[Na_2Mg_3Al_2Si_8O_{22}(OH)_2]$ and proposed a band assignment valid for richterite solid solutions of the present study; glaucophane and richterite have the same space group, $C2/m$.

High-wavenumber bands (above 600 cm^{-1}) result from vibrations involving tetrahedra. The very intense band observed at 681 cm^{-1} is assigned to the symmetrical Si-O_b-Si vibrations. The wavenumber bands above 800 cm^{-1} are principally related to Si-O_b-Si and O_b-Si-O_b asymmetrical vibrations and to Si-O_{nb} stretching vibrations [O_b, for bridging O atoms O(5), O(6), O(7) and O_{nb}, for nonbridging O atoms O(1), O(2)]. In the spectrum of Ti-free richterite, two main sharp bands are observed in this range (at 1080 and 950 cm^{-1}), with minor-intensity broad shoulders centered around 1030 and 929 cm^{-1}. A high-intensity shoulder is clearly visible at about 1090 cm^{-1} on the high-wavenumber side of the 1080 cm^{-1} band. Such high-wavenumber bands (around 1100 cm^{-1} and above) with high intensities are typical of tetrasilicic minerals with filled A sites; examples are tetrasilicic micas and amphiboles (Robert, 1988). They can be assigned to T-O$\perp$ stretching vibrations, corresponding to very short T-O$\perp$ bonds; $\perp$ means that the vibrations are approximately perpendicular to the plane of layering in micas (001) and to the plane of the double chain in amphiboles (100). In the present case, it seems reasonable to assign this high-wavenumber, high-intensity band to the stretching vibration of the T(1)-O(1) bond, since T(1)-O(1) is a very short Si-O bond in Ti-free potassic richterite (1.599 Å, Papike et al., 1969), perpendicular to the (100). In the wavenumber range below 600 cm^{-1}, the bands result from angular distortions of the double chain and from valence vibrations (stretching) in the high-coordination polyhedra, that is, in M and A sites.

For spectra of samples along the join richterite–titanium richterite, the low-wavenumber region (below 600 cm^{-1}) remains essentially unchanged, whereas significant modifications are observed in the high-wavenumber region (above 600 cm^{-1}). In this range, new bands appear whose intensity increases with increasing Ti content: a sharp band at 897 cm^{-1} and broad bands and shoulders at 853, 839, and 779 cm^{-1}. Furthermore, the intensity of the band at 926 cm^{-1} increases significantly, suggesting the superposition of two bands: the band previously observed at 929 cm^{-1} in the Ti-free richterite end-member and a new band generated by the Ti substitution. The intensity of the main high-wavenumber band (1080 cm^{-1})

remains approximately constant; only a minor shift to 1074 cm^{-1} is observed (Fig. 3).

The general features of spectra in the high-wavenumber range suggest a correspondence between the main new bands and those observed in the Ti-free richterite endmember. The new sharp band at 897 cm^{-1} can be related to the band at 950 cm^{-1} in the spectrum of the Ti-free richterite; the shift factor, calculated as the ratio 897/950, is 0.94. Similarly, the new band at 926 cm^{-1} corresponds to the band at 1030 cm^{-1} (926/1030 = 0.90), and the new broad band centered around 850 cm^{-1} corresponds to the broad band at 929 cm^{-1} in the spectrum of Ti-free richterite (850/929 = 0.92). These ratios are not fortuitous; they closely correspond to the calculated ratio from the reduced masses, μ, of the couples Si-O and Ti-O: $(\mu_{Si\text{-}O}/\mu_{Ti\text{-}O})^{1/2} = 0.92$, with $\mu_{A\text{-}B} = m_A \cdot m_B/(m_A + m_B)$. From these observations, we conclude again that Ti^{4+} is absent from octahedral sites and substitutes for [4]Si in potassium richterite.

The constant intensity of the high-wavenumber band (1080 cm^{-1}) and its small shift to 1074 cm^{-1} with Ti substitution deserve comment. According to previous observations, a new band at 994 cm^{-1} should be expected (calculated value assuming 0.92 as the theoretical wavenumbers ratio); it is not observed (Fig. 3), indicating that this band is not affected by the [4]Si → [4]Ti substitution. On the basis of crystal structure refinements, Ungaretti (1980) alloted Ti^{4+} to the T(2) tetrahedron in natural Ti-bearing potassic richterite; therefore, no major change is expected for the 1080 cm^{-1} band, since we have assigned this band to T(1)-O(1) vibrations. The origin of the minor shift may be in minor changes in the geometry of tetrahedron T(1).

The new weak broad band at 779 cm^{-1} (Fig. 3) is evidently related to Ti, since it is not visible in the spectrum of Ti-free richterite, but it cannot be related to any band observed in the spectrum of the Ti-free richterite endmember. Therefore, no satisfactory explanation of this weak band can be offered now. However, it could be caused by a very long Ti-O bond; in tetrahedron T(2), for example, the T(2)-O(6) bond is significantly longer than other T-O bonds in potassium richterite (Papike et al., 1969).

Conclusions

The substitution limit of Ti in potassium richterite observed during this study ($0.6 \leq Ti < 0.8$ Ti apfu) closely agrees with the compositional data given by several authors for natural potassium richterite (Mitchell and Lewis, 1983; Wagner and Velde, 1986; Thy et al., 1987); these extensive data are consistent in indicating a maximum content of 0.6–0.7 apfu. Ti in amphiboles can be regarded as a promising geothermometer, since its substitution limit increases drastically with increasing temperature; this makes it necessary to define the role played by Fe in the substitution of Ti. This increase in the substitution limit with increasing temperature has already been recognized in micas: phlogopite (Robert, 1976), biotite (Abrecht and Hewitt, 1988), and muscovite (Monier and Robert, 1986). There is strong evidence that increasing Fe content facilitates substitution of Ti in ferromagnesian micas (Czamanske and Wones, 1973; Abrecht and Hewitt, 1988), but no equivalent data are available for amphiboles. Likewise, no experimental data are available on the effect of pressure on Ti substitution in potassium richterite, but there are indications that pressure causes a decrease in the limits of substitution. In fact, all natural occurrences of Ti-rich potassium richterite are from rocks that crystallized under near-surface conditions (Wagner and Velde, 1986) or, at most, under 1–2 kbar pressure (Thy et al., 1987). The negative pressure dependence of Ti substitution has been recognized by Oba et al. (1982) in natural as well as synthetic kaersutite. It is also well known in synthetic phlogopite (Robert, 1976; Foley, 1990).

The various amphiboles and micas exhibit very different substitutional schemes involving Ti, as noted in references cited above and in this work. However, it is interesting to observe that the effects of temperature and pressure on substitution of Ti are qualitatively the same, whatever the substitutional mechanism.

All data provided by XRD, FTIR absorption, and Raman scattering spectroscopy, as well as recent EXAFS and XANES spectroscopic data obtained for the synthetic samples described in the present work (Mottana et al., 1990; Paris et al., 1990) collectively demonstrate that Ti^{4+} is tetrahedrally coordinated and replaces Si^{4+} in potassic richterite. Tetrahedral coordination of Ti^{4+} is uncommon in silicates and in other compounds. Among silicates, only garnets have significant amounts of [4]Ti^{4+} (see Waychunas, 1987, for a compilation). Trace amounts of [4]Ti apparently replace [4]Si in diopside (Carbonin et al., 1989). The rare mineral sillenite $Bi_{12}O_{18}\cdot(Si,Ti)O_2$ (Tarte, personal communication, 1988) is a third example of that substitution. A few nonsilicates also contain [4]Ti^{4+} as a major component, including Ba_2TiO_4 (Tarte, 1961), Rb_2TiO_3 (Schartau and Hoppe, 1974), and NiTi spinels (Lager et al., 1981). Potassium richterite is therefore the first clearly defined example of a polymerized silicate containing [4]Ti^{4+} as a major component.

Acknowledgments

This work was carried out during the visit of G.D.V. to the CNRS-BRGM Research Center in Orléans, France and was financially supported by a CNR-NATO grant and by a MPI Cristallochimica e Petrogenesi grant. Sincere thanks are due to M. Lagache, J. Fabriès, and Z. Johan for allowing the visit of G.D.V. to their laboratories and for encouragement and suggestions. J. Calas assisted with the use of FTIR facilities. Helpful suggestions of F.C. Hawthorne, A. Mottana, F. Seifert, C. Ross II, L. Ungaretti, P. Tarte, and referee A.C. Turnock improved the manuscript.

References cited

Abrecht, J., and Hewitt, D.A. (1988) Experimental evidence on the substitution of Ti in biotite. American Mineralogist, 73, 1275–1284.

Appleman, D.E., and Evans, H.T., Jr. (1973) Job 9214: Indexing and least-square refinement of powder diffraction data. U.S. Department of Commerce, National Technical Service Publication PB 216-188.

Cameron, M., Sueno, S., Papike, J.J., and Prewitt, C.T. (1983) High tem-

perature crystal chemistry of K and Na fluor-richterite. American Mineralogist, 68, 924–935.

Carbonin, S., Salviulo, G., Munno, R., Desiderio, M., and Dal Negro, A. (1989) Crystal-chemical examination of natural diopsides: Some geometrical indications of Si-Ti tetrahedral substitution. Mineralogy and Petrology, 41, 1–10.

Carmichael, I.S.E. (1967) The mineralogy and petrology of the volcanic rocks from the Leucite Hills, Wyoming. Contributions to Mineralogy and Petrology, 15, 24–66.

Charles, R.W. (1975) The phase equilibria of richterite and ferrorichterite. American Mineralogist, 60, 367–374.

Czamanske, G.K., and Wones, D.R. (1973) Oxidation during magmatic differentiation, Finnmarka complex, Oslo area, Norway: Part 2, The mafic silicates. Journal of Petrology, 14, 349–380.

Della Ventura, G., and Robert, J.-L. (1990) Synthesis, XRD and FTIR studies of strontium richterites. European Journal of Mineralogy, 2, 171–175.

Docka, J.A., Post, J.E., Bish, D.L., and Burnham, C.W. (1987) Positional disorder of A-site cations in *C2/m* amphiboles: Model energy calculations and probability studies. American Mineralogist, 72, 949–958.

Dubeau, M.L., and Edgar, A.D. (1985) Priderite stability in the system $K_2MgTi_7O_{16}$-$BaMgTi_7O_{16}$. Mineralogical Magazine, 49, 603–606.

Foley, S.F. (1990) Experimental constraints on phlogopite chemistry in lamproites: 2. Effect of pressure-temperature variations. European Journal of Mineralogy, 2, 327–341.

Forbes, W.C., and Flower, M.F.J. (1974) Phase relations of titan-phlogopite, $K_2Mg_4TiAl_2Si_6O_{20}(OH)_4$, a refractory phase in the upper mantle? Earth and Planetary Science Letters, 22, 60–66.

Gillet, Ph., Reynard, B., and Tequi, C. (1989) Thermodynamic properties of glaucophane. New data from calorimetric and spectroscopic measurements. Physics and Chemistry of Minerals, 16, 659–667.

Hamilton, D.L., and Henderson, C.M.B. (1968) The preparation of silicate compositions by a gelling method. Mineralogical Magazine, 36, 832–838.

Hartman, P. (1969) Can Ti^{4+} replace Si^{4+} in silicates? Mineralogical Magazine, 37, 366–369.

Hawthorne, F.C. (1981) Crystal chemistry of the amphiboles. In Mineralogical Society of America Reviews in Mineralogy, 9A, 1–102.

Helz, R.T. (1973) Phase relations of basalts in their melting range at PH_2O = 5 kb as a function of oxygen fugacity. Part I. Mafic phases. Journal of Petrology, 14, 249–302.

Huebner, J.S., and Papike, J.J. (1970) Synthesis and crystal chemistry of sodium-potassium richterites $(Na,K)NaCaMg_5Si_8O_{22}(OH,F)_2$: A model for amphiboles. American Mineralogist, 55, 1973–1992.

Huggins, F.E., Virgo, D., and Huckenholz, H.G. (1977) Titanium containing silicate garnets II. The crystal chemistry of melanites and schorlomites. American Mineralogist, 62, 646–665.

Jaques, A.L., Lewis, J.D., Smith, C.B., Gregory, G.P., Ferguson, J.F., Chappell, B.W., and McCulloch, M.T. (1984) The diamond-bearing ultrapotassic (lamproitic) rocks of the West Kimberley region, Western Australia. In J. Kornprobst, Ed., Kimberlites, I: Kimberlites and related rocks, p. 225–254. Elsevier, Amsterdam.

Kitamura, M., Tokonami, M., and Morimoto, N. (1975) Distribution of titanium atoms in oxy-kaersutite. Contributions to Mineralogy and Petrology, 51, 167–172.

Kuehner, S.M., Edgar, A.D., and Arima, M. (1981) Petrogenesis of the ultrapotassic rocks from the Leucite Hills, Wyoming. American Mineralogist, 66, 663–677.

Lager, G.A., Armbruster, T., Ross, F.K., Rotella, F.J., and Jorgenson, J.D. (1981) Neutron powder diffraction study of defect spinel structures: Tetrahedrally coordinated Ti^{4+} in $Ni_{2.62}Ti_{0.69}O_4$ and $Ni_{2.42}Ti_{0.74}Si_{0.05}O_4$. Journal of Applied Crystallography, 14, 261–264.

Mitchell, R.H., and Lewis, R.D. (1983) Priderite-bearing xenoliths from the Prairie Creek mica peridotite, Arkansas. Canadian Mineralogist, 21, 59–64.

Monier, G., and Robert, J.-L. (1986) Titanium in muscovite from two mica granites: Substitutional mechanism and partition with coexisting biotites. Neues Jahrbuch für Mineralogie Abhandlungen, 153, 147–161.

Moore, P.B. (1969) Joesmithite: A novel amphibole crystal chemistry. Mineralogical Society of America Special Papers, 2, 111–115.

Mottana, A., Paris, E., Della Ventura, G., and Robert, J.-L. (1990) Spectroscopic evidence for tetrahedrally-coordinated titanium in richteritic amphiboles. Rendiconti Lincei, Scienze Fisiche e Naturali, Series 9, 1, 387–392.

Oba, T., Yagi, K., and Hariya, Y. (1982) Stability relation of kaersutite, reinvestigated on natural and synthetic samples. XIIIth General Meeting I.M.A., Varna, Bulgaria, 282.

Papike, J.J., Ross, M., and Clark, J.R. (1969) Crystal-chemical characterization of clinoamphiboles based on five new structure refinements. Mineralogical Society of America Special Paper, 2, 117–136.

Paris, E., Mottana, A., Della Ventura, G., and Robert, J.-L. (1990) Valenza e coordinazione del titanio in anfiboli sintetici della serie richterite—Ti-richterite. Studio XANES in luce di sincrotrone (abs.). Plinius, 3, 81–82.

Prider, R.T. (1939) Some minerals from the leucite-rich rocks of the West Kimberley area, Western Australia. Mineralogical Magazine, 25, 373–387.

Raudsepp, M., Turnock, A.C., Hawthorne, F.C., Sheriff, B.L., and Hartman, J.S. (1987) Characterization of synthetic pargasitic amphiboles $(NaCa_2Mg_4M^{3+}Si_6Al_2O_{22}(OH,F)_2$; M^{3+} = Al, Cr, Ga, Sc, In) by infrared spectroscopy, Rietveld structure refinement, and ^{27}Al, ^{29}Si, and ^{19}F MAS NMR spectroscopy. American Mineralogist, 72, 580–593.

Robert, J.-L. (1976) Titanium solubility in phlogopite solid solutions. Chemical Geology, 17, 213–227.

——— (1981) Études cristallochimiques sur les micas et les amphiboles. Applications pétrographiques et géochimiques, 206 p. Thèse d'Etat, Université Paris XI, Paris.

——— (1988) Relationships between Raman and IR studies in silicates, with special reference to layer and chain silicates (abs.). European Meeting on "Absorption Spectroscopy in Mineralogy." Rome, Italy.

Robert, J.-L., and Kodama, H. (1988) Generalization of the correlations between hydroxyl-stretching wavenumbers and composition of micas in the system K_2O-MgO-Al_2O_3-SiO_2-H_2O: A single model for trioctahedral and dioctahedral micas. American Journal of Science, Wones Volume, 288-A, 196–212.

Robert, J.-L., Della Ventura, G., and Thauvin, J.-L. (1989). The OH-stretching region of synthetic richterites in the system Na_2O-K_2O-CaO-MgO-SiO_2-H_2O-HF. European Journal of Mineralogy, 1, 203–211.

Schartau, W., and Hoppe, R. (1974) Rb_2TiO_3, ein neues Oxotitanat mit der Koordinationszahl 4. Zeitschrift für Anorganische und Allgemeine Chemie, 408, 60–74.

Seifert, F., and Schreyer, W. (1971) Synthesis and stability of micas in the system K_2O-MgO-SiO_2-H_2O and their relations to phlogopite. Contributions to Mineralogy and Petrology, 30, 196–215.

Semet, M.P. (1973) A crystal-chemical study of synthetic magnesiohastingsite. American Mineralogist, 58, 480–494.

Shannon, R.D. (1976) Revised effective ionic radii and systematic studies of interatomic distances in halides and chalcogenides. Acta Crystallographica, A32, 751–767.

Shimazaki, H., Bunno, M., and Ozawa, T. (1984) Sadanagaite and magnesio-sadanagaite, new silica-poor members of calcic amphibole from Japan. American Mineralogist, 69, 465–471.

Tarte, P. (1961) Infra-red spectroscopic evidence of four-fold co-ordination of titanium in barium orthotitanate. Nature, 191, 1002–1003.

Tateyama, H., Shimoda, S., and Sudo, T. (1976) Infrared absorption of synthetic Al-free magnesium micas. Neues Jahrbuch Mineralogie Monatshefte, 3, 128–140.

Thy, P., Stecher, O., and Korstgård, J.A. (1987) Mineral chemistry and crystallization sequences in kimberlite and lamproite dikes from the Sisimiut area, central West Greenland. Lithos, 20, 391–417.

Ungaretti, L. (1980) Recent developments in X-ray single crystal diffractometry applied to the crystal-chemical study of amphiboles. Godišnjak Jugoslavenskog centre za kristalografiju, Zagreb, 15, 29–65.

Wagner, C., and Velde, D. (1986) The mineralogy of K-richterite-bearing lamproites. American Mineralogist, 71, 17–37.

Waychunas, G.A. (1987) Synchrotron radiation XANES spectroscopy of Ti in minerals: Effects of Ti bonding distances, Ti valence, and site geometry on absorption edge structure. American Mineralogist, 72, 89–101.

Manuscript received July 27, 1990
Manuscript accepted April 5, 1991